PROCEEDINGS, Thirty-Seventh Workshop on Geothermal Reservoir Engineering
Stanford University, Stanford, California, January 30 - February 1, 2012
SGP-TR-194

DEVELOPMENT OF A NEW TEMPERATURE CONTROLLED TRUE-TRIAXIAL APPARATUS FOR SIMULATING ENHANCED GEOTHERMAL SYSTEMS (EGS) AT THE LABORATORY SCALE

Luke P. Frash and Marte Gutierrez

Colorado School of Mines
1610 Illinois St.
Golden, CO, 80401, USA
E-mail: lfrash@mines.edu

ABSTRACT

The prediction of hydraulically induced fractures and the characterization of these fractures for fluid flow and heat transfer is a limiting factor in the development of Enhanced Geothermal Systems (EGS) technology. To study hydraulically induced fractures in crystalline rock reservoirs, a new true-triaxial apparatus was developed and tested.

The apparatus is capable of applying three independently controlled principal stresses up to 12 MPa and temperatures as high as 180 °C to a 30x30x30 cm cubical rock sample. Hydraulic fracturing is performed from hydraulic tubing installed in 10 mm oriented boreholes which are drilled into a pressurized sample. Fracturing fluid pressures up to 70 MPa can be applied with volumetric flow rates as low as 0.00001 mL/min allowing for high strength rocks to be fractured and fracture extents to be contained within the 30 cm sample. With a second borehole drilled to intercept the induced fracture, fluid circulation experiments are performed to characterize the thermal properties of the reservoir. Sensor systems measure temperatures, pressures, flow rates, and strains such that the fluid state and rock loading parameters can be monitored for use in the validation of a computer model currently being developed.

Initial testing has been performed on an artificial granite sample to calibrate the system. The artificial granitite sample is created using a specialized high performance concrete designed to replicate Colorado Red Granite as available from local quarries. Using fine aggregate silica fume concrete allows for the creation of cast homogenous samples with a greater uniformity of axial stress distributions and controllable internal discontinuities. Tested parameters for characterizing the rock include unconfined compressive strength, indirect tensile strength, mode I fracture toughness, elastic modulus, thermal conductivity, specific heat capacity, coefficient of thermal expansion, porosity and permeability.

The triaxial system is designed to allow for future application of acoustic emission (AE) fracture monitoring for relating the laboratory data to field tests and a proppant injection system will also be applied to analyze the effect of proppant and high viscosity fluid injections on the fracture thermal characteristics.

INTRODUCTION

In the application of geothermal energy technology to EGS systems, there are many significant difficulties limiting the ability to predict system performance prior to site development and production. These issues are well documented in the MIT led report, "The Future of Geothermal Energy." (Tester et. al., 2006). Of these difficulties, our limited ability to predict hydraulic fracture geometries and estimate their heat exchange properties is of particular interest to this research project.

To gain a better understanding of the behavior of hydraulic fracturing treatments in EGS application, a new temperature controlled true-triaxial apparatus has been developed. This device allows for EGS hydraulic fracturing treatments to be simulated at the laboratory scale with oriented single or binary well configurations. Also, the apparatus has been developed to allow for boreholes to be drilled while the sample is fully loaded with confining stresses and heated. Data acquisition systems have been installed to allow for multi-point real-time process monitoring of hydraulic fracturing and fluid circulation stages, the stress and temperature state of the sample, and the acoustic emissions (AE) geometric profile of the stimulated fracture. Overall, this system is capable of closely simulating a field EGS treatment for a geothermal anomaly at a temperature of up to 180 ºC and depth of roughly 460 m. The data produced from fracturing experiments performed using this apparatus is intended to be compatible with field

data. Also, a full materials testing program has been planned to provide information on the sample characteristics as would be applicable to thermo-mechanical models. Ultimately, the data produced from these experiments will be used in the validation of a new advanced stimulation prediction model with true three dimensional capabilities being developed in tandem with this project. Also the results of this project are expected to provide some additional insight into the hydraulic fracturing process as used in EGS technology applications.

EQUIPMMENT DEVELOPED

The full system used to perform the laboratory scale EGS fracturing tests has been developed as several integrated subsystems. Each of these has been described in detail within this section.

True Triaxial Cell

A custom load cell has been developed to allow for the simulation of the EGS environment at the laboratory scale. Images of this load cell are provided in Figure 1 and Figure 2 in an unloaded and loaded configuration respectively.

Figure 1: Unloaded heated true-triaxial load cell.

Figure 2: Loaded cell with borehole being drilled using the oriented drilling rig.

This loading cell is capable of applying three independently-controlled principal stresses to a cubical sample at up to 12.2 MPa for a 30x30x30 cm size. The confining stresses are applied using three Freyssinet 350 mm steel flat jacks and Enerpac P80 hydraulic hand pumps. This true-triaxial loading method has been proven to be effective by past research (Behrmann and Elbel, 1991; Rawlings et. al., 1993; Savic et. al., 1993; Mogi, 2007) and is considered to be more economical than a three-axis hydraulic load frame. To provide a reaction frame for the applied horizontal stresses, the flat jack system is supported by a cylindrical pressure vessel structure with a steel fiber reinforced medium-strength concrete backing. This concrete backing allows for a square aperture and the ability to load cubical samples. For the vertical stresses, an A514 high strength low-alloy 50 mm thick steel lid is used with an open port in the top lid to allow for passage of hydraulic lines and signal cables. This lid is installed blank so boreholes into the sample may be drilled through the lid while fully loaded at a user-selectable orientation to access the sample.

To apply heating, a dual-zone 3600 W flexible silicone heater system has been installed on the external surface of the cell. Each zone of heating consists of two 900 W heater elements controlled by a proportional-integral-derivative (PID) device. These zones are located on the sides and bottom of the cell respectively to allow for potential simulation of lateral and deep heating thermal recharge of the reservoir. In the field, lateral thermal recharge would be expected to be dominated by conduction of existing heat from lateral rock sources while the deep thermal recharge is driven by the vertical temperature gradient and the radioactive thermal generation produced in basement rock formations (Beardsmore, 2001).

For the borehole, a 10 mm diameter bore is installed using a custom drill press. The 10 mm diameter was selected in an attempt to create a scaled EGS binary well circulation system within a single sample block. The borehole is installed using a Bosch 11224VSRC rotary hammer drill mounted to a rigid screw-feed drill press with 300 mm of travel. This configuration allows for a high accuracy oriented borehole to be drilled through the steel lid and into the rock sample.

Hydraulic Fracturing System

The hydraulic system used to perform fracturing and fluid circulation operations has been developed to provide a similar functionality to the equipment used in the field. The primary functions replicated include high precision constant flow rate control, continuous flow high viscosity fluid pumping capability, and a controlled concentration proppant slurry injection system. Together, these elements allow for the generation of controlled length propped fractures and are intended to be used to create a laboratory scale EGS system. A diagram of the full hydraulic system is provided in Figure 3.

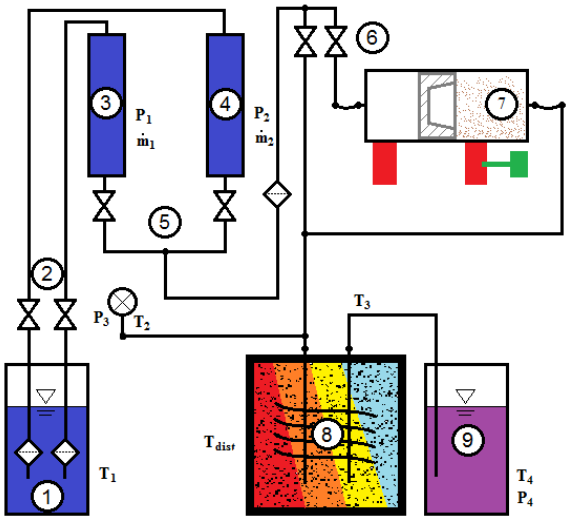

Figure 3: Diagram for the hydraulic fracturing system showing the inflow fluid reservoir (1), pneumatic actuated continuous flow valve system (2 and 5), dual high pressure syringe pumps (3 and 4), clean to slurry valve switching system (6), rotationally mixed hydraulic to hydraulic piston actuator, sample block (8), outflow reservoir (9), and general arrangement of sensor systems.

In this system, a dual Teledyne Isco 65DM syringe pump system was selected to achieve a precision continuous flow rate with high pressure capability. This system allows for controlled flow rates of 25 to 0.00001 mL/min with an accuracy of ± 0.3% from the set point per the manufacturer. During the hydraulic fracturing process, flow rates in the range of 0.01 to 5 mL/min are expected to be adequate for generating controlled length fractures fully contained within the sample block. These limit values were determined using Perkins and Kern hydraulic fracturing model estimations (Kumar, 2011) and experimental data collected during calibration and design validation testing. Due to the significant scale effects present in the laboratory as compared to the field, the flow rates used are not expected to correlate directly with typical flow rates used by field pumping equipment.

With the dual pump system and an automated pneumatically actuated valve system, these two pumps allow for continuous flow operation. With this functionality, a binary EGS system can be simulated at the laboratory scale with an injection and production well. During this mode of operation, the expected injection flow rates range from 0.01 to 0.0002 mL/min as an output from the dual-pump system and are measureable with reasonable accuracy. For the outflow rate measurement and characterization of any leak-off parameters, a pressure transducer is used to monitor the fluid volume in the outflow reservoir as a function of time. This system allows for a reasonably accurate indirect measurement of the outflow rate through differential analysis where the accuracy of the system is a function of the outflow reservoir dimensions and instrument accuracy.

According to the literature, high viscosity injection fluids can be used to generate more controlled, shorter length, and wider aperture fractures during a treatment process (Ishida et. al., 2004). These characteristics are preferred in this laboratory application due to the small size of the sample and the benefit of generating a fully contained fracture for the purposes of EGS system simulation. Thus, the system has been designed to allow for the injection of fluids with a viscosity of up to 1000 cP. In the field, a gelling system with a cross-linking polymer can be used to generate fluids with viscosity values in this range (Franklin Well Service, 2012) and these same fluids could ideally be used in the lab as well.

To allow for the injection of high viscosity proppant slurry, a specialized rotationally-mixed liquid-liquid piston accumulator has been implemented into the system. Using this mixer allows for the abrasive proppant particles to be isolated from the wear-sensitive system components while also allowing for the implementation of a stepped proppant injection scheme as would be used in the field. To further enhance the utility of this accumulator, the device is rotated along a horizontal axis at a user-selectable speed allowing for control over the mixing efficiency. At high speeds, the device will act as a centrifuge while at lower speeds the proppant concentration output will be an experimentally calibrated function of rotation speed. Currently, the calibration procedures are not yet completed, but the expected relationship using is illustrated in Figure 4.

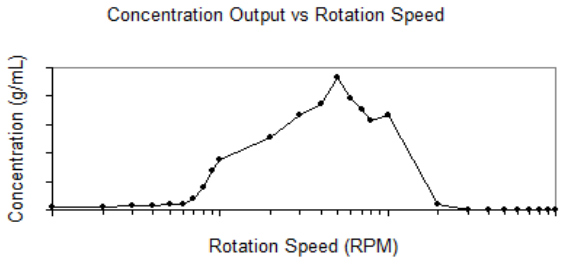

Figure 4: Expected function shape for mixer speed and concentration output.

Data Acquisition System (DAQ)

The DAQ system used to monitor and control the laboratory performed hydraulic fracturing has been designed to record all essential operating parameters as is standard for field applications while also implementing some additional elements to take

advantage of the improved accessibility that a laboratory setup allows for. At the most basic level, all EGS wells should be setup to record operating fluid pressure, flow rate, and temperature so the laboratory equipment has been instrumented to do the same. To monitor the real-time fracturing geometry, an acoustic emissions system has been implemented into the true-triaxial cell with the sensors housed in the steel pressure platens used to apply confining stresses to the samples. Also, a new spontaneous potential (SP) monitoring system is embedded into two perpendicular faces of the sample to test its potential applications for hydraulic fracture monitoring of fluid flow directions. For temperature distribution monitoring during circulation operations, a thermocouple array is installed to monitor real-time bottom hole temperature and the temperature distribution around the surface of the sample. For loading stress uniformity verifications, a strain gage rosette pattern will be installed on the surface of the sample as well.

These measurements are recorded by several DAQ systems. The primary process information is recorded by an National Instruments Compact DAQ with thermocouple, strain gage, current, and voltage modules. This DAQ collects all temperature and pressure information. The injection flow rates and pump information are recorded though the Teledyne Isco pump controller using serial connections. All AE data is collected using a standalone system provided by the Physical Acoustics Corporation. The state of the true-triaxial cell's heater system is recorded using serial connections to the PID controller.

Materials and Fluids

The hydraulic fracturing process is known to be significantly affected by the material properties of the subject media and the injected fluid characteristics. For a successful execution of controlled hydraulic fracturing in the laboratory, these properties are ideally known and consistent so that they do not act as additional unwanted variables. The ideal sample material would be homogenous and intact to allow for theoretically repeatable fractures. The ideal injection fluid would be Newtonian with predictable properties as functions of temperature and pressure which are known variables in an EGS application.

Due to the natural and mostly unpredictable non-homogenous structure of natural rock, fine aggregate concrete mixtures have been selected as the primary sample material for the initial testing with the true-triaxial cell. These materials include a medium strength concrete grout mix and an ultra-high strength concrete mix. The medium strength concrete was used for unconfined concept testing while ultra-high strength concrete was loaded inside the true-triaxial cell for systems integration testing. Quickcrete Fastset™ non-shrink grout mix was used for the medium strength concrete sample while a specialized silica fume mix was developed for the ultra-high strength sample. All concrete samples were hand mixed and cured for at least 14 days in a controlled 25 ºC 100% humidity room.

A material testing scheme has been implemented to fully characterize the mechanical, thermal, and hydraulic properties as relevant to the hydraulic fracturing process. The measured properties include uniaxial compressive strength, indirect tensile strength, Young's modulus, Poisson's ratio, internal friction angle, mode-I fracture toughness, thermal conductivity, specific heat capacity, thermal expansion coefficient, permeability, porosity, and density. When possible, the relevant ASTM standards will be followed for each of these material tests but some improvised tests were used due to limited equipment availability.

While this testing is on-going, Table 1 provides a summary of the measured and expected values for several of the key properties for each of the materials used. Completion of the remaining tests is imminent with the submission of this paper and the respective results may be provided upon request.

Table 1: Measured and expected material properties for preliminary test sample materials.

Property	Medium Strength	Ultra-high Strength
Compressive Strength† (MPa)	40*	150*
Indirect Tensile Strength‡ (MPa)	2.8	5.3
Density (Mg/m^3)	2.08	2.14

* Expected value not yet verified by measurements
† Performed following ASTM D7012
‡ Performed following ASTM D3967

Recognizing the lack of an accepted standard for mode-I fracture toughness measurement with concrete or rock materials, a simple notched beam fracture toughness testing apparatus has been developed as auxiliary equipment for this project. Figure 5 provides an image of this equipment being used in a three-point loading configuration for short beam samples. The equipment developed has been designed to load small beam samples with a depth of 25 to 50 mm and a length of 120 to 250 mm. To concentrate the stresses, a controlled depth

perpendicular slot is cut across the bottom face of the beam using a carbide saw with a depth guide. Classical moment based linear-elastic fracture mechanics theory is used to obtain an estimate of the fracture toughness (Dubynas, 1999).

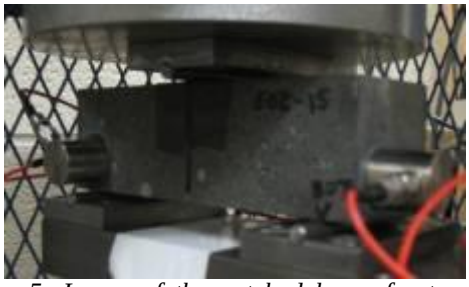

Figure 5: Image of the notched beam fracture test being performed on a short beam sample with a three-point loading configuration.

The fluids used for the initial fracturing tests included distilled water and a simple brine solution. These fluids were selected for ease of access and their well known hydraulic and thermodynamic properties. The brine was mixed using plain table salt and distilled water at concentrations ranging from 2.5 to 10.0 g/L. All testing performed with the new SP monitoring system used a brine solution to improve the strength of the electrical signals produced by the fluid flow. The fluids were injected at an average room temperature of 24 ºC.

Systems Interfacing

Three key design elements were developed to allow for the different systems to be functionally integrated. First, a large port was installed in the top lid of the true-triaxial cell to allow for passage of hydraulic lines and internal instrument cables. Second, fittings were installed on the hydraulics system to allow for pressure and temperature monitoring. Third, a specialized borehole sealing system was developed to allow for the hydraulic fluid to be injected into the drilled borehole without leakage to the environment.

For the borehole sealing system, several different methods were considered including grouted casing with perforations, flexible packer systems, and simple drill through open borehole systems. Each of the proposed systems were tested in the validation experiments, or eliminated using theoretical analysis, to determine the system that generated the most reliable seal and provided an isolated fracturing interval with the maximum possible predictability.

A literature review was performed to evaluate the effectiveness of a perforated casing system as compared to an open borehole option. In typical field hydraulic fracturing, such as performed by the oil and gas industry, a steel casing is installed in the borehole and perforated using explosives or water jet cutting (Daneshy, 1973; Smith et. al., 2008). However, laboratory studies have shown open boreholes to produce more predictable fractures with lower near wellbore tortuosity as the fluid follows a more direct flow path with the opening of the fracture in a perpendicular direction to the far field minimum principal stress Thus, for the small scale fractures being generated in this project an open borehole fracturing interval was found to be preferred. Using an open borehole is also expected to result in a larger effective hydraulic fracturing length with a deeper proppant penetration due to the reduced constrictions present with a high near wellbore tortuosity.

With this choice, borehole stability issues become a greater concern as the lack of a supporting casing increases the probability of a borehole breakout. To minimize the chance of a borehole stability failure, the confining stresses are kept below the theoretical limit predicted by linear elastic stress theory and the Kirsch solution for near bore stresses (Valkó and Economides, 1995).

The most effective method for sealing the hydraulic casing into the borehole was found to be achievable with the design shown in Figure 6. This design utilizes externally threaded thick walled seamless drawn carbon steel tubing with an outside diameter of 8 mm, wall thickness of 2.5 mm, and external thread of ¼”-20. The threaded casing is grouted into the 10 mm borehole, as drilled by the rotary hammer drill press into the sample, for a minimum length of 50 mm. After allowing for adequate cure time, a smaller diameter 2.4 mm (3/32”) bore is drilled internally through the casing to create an uncased fracturing interval beneath the grouted casing. Several precursors to this design variant were tested on an unconfined sample, including both perforated and drill-through options, before arriving at this final concept. These tests and their findings will be discussed in the following sections.

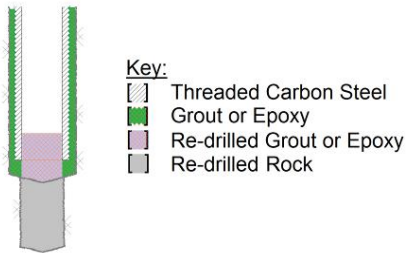

Figure 6: Threaded drill-through borehole sealing system with open bore fracturing interval.

PRELIMINARY CALIBRATION RESULTS

The preliminary testing included several concept validation tests and a full systems integrations test. The concept validation tests were performed to experiment with different borehole sealing methods,

to calibrate the AE monitoring system, and to provide concept testing data for the SP monitoring system. The full systems integration test was used to validate the planned experimental procedure for all stages of the laboratory scale EGS fracturing treatment from sample loading to post-test sample dissection analysis.

Systems Integration Test

For the system integration test, a ultra-high strength concrete sample was loaded into the true-triaxial cell and drilled while horizontally pressurized. The applied stresses were held constant at 0, 3.1, and 6.1 MPa for the vertical, minimum horizontal, and maximum horizontal stresses respectively. A single vertical borehole was drilled through the center of the sample and subjected to three different sealing configurations. The initial drilled borehole depth was 179 mm from the surface of the sample. A total of 11 attempted fracturing treatments were performed with the results as given in Table 2. A verifiable fracturing event was not observed until attempt 10.

Table 2: Results of fracturing attempts during the systems integration test.

Attempt #	Config.	Flowrate (mL/min)	Breakdown (kPa)	Fracture (Y/N)
1	A	0.05	15247	N
2	A	0.15, 0.3, 1.0, 2.0, 5.0, 10.0	20508	N
3	A	0.02	15457	N
4	A	0.02	13155	N
5	B	0.05	11991	N
6	B	0.1	12286	N
7	B	0.5	17411	N
8	C	0.05	13329	N
9	C	0.1	12388	N
10	C	0.5	8869	Y
11	C	0.5	8643	Y
12	C	1.0	9246	Y

In the table, Configuration A used a simple straight tubing section grouted into the sample block with epoxy. The tubing was drawn seamless stainless steel with an outside diameter of 9.52 mm (3/8”) and an inside diameter of 6.35 mm. The tubing was perforated with two coaxial 1.59 mm (1/16”) holes through the diameter of the tubing at 13 mm from the embedment end, as shown in Figure 7. The end of the tubing was filled with an epoxy plug having a length of at least 6 mm which was allowed to cure before embedment to create a hydraulic seal. The perforations were pre-filled with wax in an attempt to prevent epoxy grout from entering the borehole during the sealing process. To seal the tubing into the borehole, a Loctite 5-Minute epoxy system was used with down hole delivery and mixing. A plastic capsule delivery system allowed for insertion of the unmixed two-part epoxy into the bottom of the borehole. The mixing was performed by mashing the capsules with the plugged and perforated tubing end and spinning.

Figure 7: Image of the perforated borehole casing used for the systems integration test with wax plugged perforations.

With Configuration A installed, fracturing attempts 1 through 4 were executed to test the behavior of the system and attempt to create a fracture. Attempts 1 and 2 were performed within 5 hours of the grouting procedure while attempts 3 and 4 were performed the following day to allow for the full recommended 24 hour epoxy cure. After observing an unexpected fluctuating pressure behavior with multiple peaks occurring at a given flow rate, as shown in Figure 8, it was concluded that no hydraulic fracturing of the concrete sample had occurred.

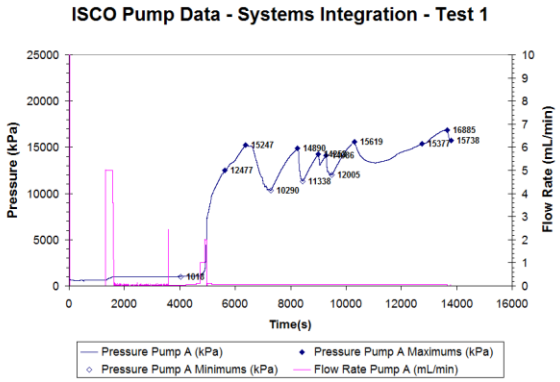

Figure 8: Pressure-time plot for the first fracture attempt for the systems integration test.

Next, the Configuration B sealing system was implemented using an extended range close tolerance drill bit to clear any epoxy away from the perforated zone, which was suspected of infiltrating into the casing during the grouting procedure, and potentially establish hydraulic fluid access to the sample material. Fracturing attempts 5 through 7 were performed with this configuration. All three of these attempts showed similar behavior to attempts 1 though 4 and also did not positively indicate that hydraulic fracturing of the sample had occurred.

Configuration C was then implemented where the epoxy plug was drilled through to bypass the perforated zone and provide hydraulic fluid access to sample material at the base of the casing system. With this final configuration, fracturing attempts 8 though 12 were performed. During fracturing attempts 8 and 9, a new asymptotic pressure behavior was observed indicating a borehole behavior different from attempts 1 through 7. In fracturing attempts 10 though 12, a distinctive hydraulic fracturing pressure plot was produced indicating the successful generation of a hydraulic fracture. Figure 9 provides a plot of the pressure-time data as observed during attempts 10 and 11. This plot shows the typical pressure build up, rapid breakdown, and fracture extension behavior expected for a successful hydraulic fracturing treatment (ASTM D4645).

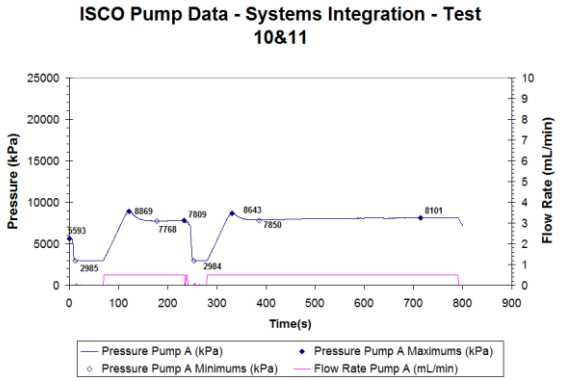

Figure 9: Pressure-time plot produced from the successful hydraulic fracture generated during attempts 10 and 11 of the systems integration test.

The fracture generated during the systems integration test used a sufficient flow time to ensure that the fracture would extend to the surface of the sample. This was done to allow for the creation of a large easily located fracture plane for post-test geometric analysis. To analyze the fracture geometry, the sample was initially cored to remove the steel casing and provide an estimate for the fracturing direction. A diamond table saw with a 915 mm diameter blade was then used to cut cross sections from the fractured sample block. The large fracture traces were easily identified on the cut sections and fine fractures were located by sanding the faces, wetting them, and rapidly drying them with a heat gun to expose the fracture traces in the sample. Figure 10 illustrates the fracture geometry as seen on a cross-section taken through the core location. The cross-section was cut parallel with the minimum horizontal confining stress direction so as to best show the hydraulic fracture profile. In this test, the fracture was found to extend perpendicular to the minimum principal stress as expected by common hydraulic fracturing theory.

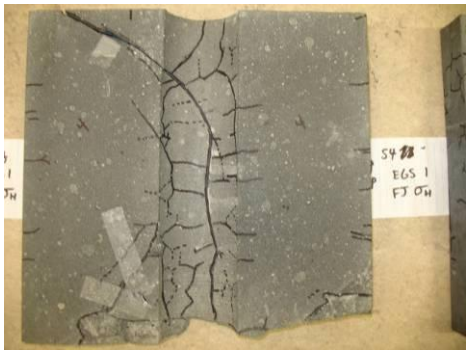

Figure 10: Cross-section of the sample fractured during the systems integration test. The observed fracture traces are marked with black ink for better visibility.

From visual analysis of the cross sections, multiple fractures were observed within and on the surface faces of the sample. While there was some uncertainty in the dimensions of the fracture traces, one of the larger fracture traces was found to intersect the injection point while also extending through the entire length of the sample. This prominent fracture was assumed to be hydraulically created as no dye system had been used to mark the flow of the fracturing fluid and no AE data had been recorded during this test. Figure 11 illustrates the expected hydraulic fracturing geometry inside of the sample. This geometry was found to be notably complex as compared to the simplistic bi-wing planar geometry typically assumed by hydraulic fracture models. Also, a distinctive splitting of the fracture can be observed in this image. This figure was formed from compiled fracture traces through consecutive cross sections.

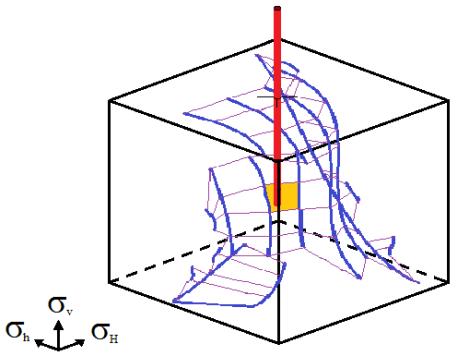

Figure 11: Diagram of the observed hydraulic fracture geometry as estimated from visual cross section analysis.

Additional observations of interest were made during the visual analysis of the fractures concerning sample damage due to coring and surface fracture networks. In both the sample core and the cross sections cut near the coring location, small but numerous lateral

fractures were observed perpendicular to the coring direction. While it is known that coring does cause damage to the sample material (Hunt, 2005), the cross section shows that similar damage was occurring in the formation as well. As seen in Figure 10, these mechanically induced fractures were found to have typical lengths of 0 to 38 mm. Also, some fractures were found to be symmetric across the bore axis while others were not. For the surface fracture networks, as shown in Figure 12, all of these fractures were found to be relatively shallow at less than 50 mm in depth. Near the surface, the hydraulic fracture appeared to have intersected one of these surface fractures to allow for restricted fluid exit flow from the sample.

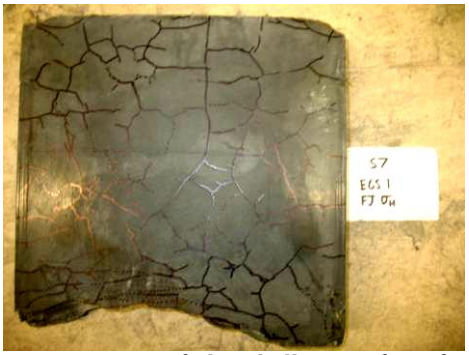

Figure 12: Image of the shallow surface fracture network observed on the external face of the sample.

Concept Validation Tests

After the systems integration test was completed, several concept validation tests were executed to test additional borehole sealing methods and provide opportunities for calibrating the AE and SP monitoring systems. All of the validation tests were performed using an unconfined 30x30x28 cm block of medium strength concrete. An image of the test block with sensors attached is shown in Figure 13. A total of six AE sensors were installed over three sample faces using the same configuration as the true-triaxial cell. Two 4x4 SP sensor grids were installed on two perpendicular faces of the sample. A total of 12 vertical boreholes and 1 oriented borehole at 25º from vertical were drilled into the sample to a nominal depth of 200 mm.

Figure 13: Instrumented medium strength concrete sample block used for concept validation testing.

Ultimately, these validation tests were used to refine the borehole sealing methods to the method shown in Figure 6. In these tests, it was observed that stainless steel tubing resulted in a poor hydraulic seal regardless of the grouting compound used. Also, a method to identify borehole seal failure through the shape of the pressure-time plot was identified. In all instances of seal failure, the pressure plot was characterized by a decreasing slope after linear segment during the pressurization stage at constant flow rate. With a successful hydraulic fracture event, the pressure would increase at a nearly linear rate until an abrupt pressure decrease was observed indicating brittle failure and hydraulic fracture initiation.

SUMMARY

This new true-triaxial apparatus has been developed to allow for laboratory scale simulation of EGS fracturing and fluid circulation. The apparatus is capable of performing hydraulic fracturing treatments on cubical sample specimens while also applying independently controlled principal confining stresses and heat. General features and specification for the equipment include:

- 30x30x30 cm cubical sample size
- Confining stresses of up to 12.2 MPa applied by flat jacks
- Heating up to 180 ºC
- Orientated boreholes drillable into stressed and heated samples

- 10 mm borehole diameter
- Threaded carbon steel casing system with down hole grout delivery using capsules
- Perforated or uncased hydraulic fracturing interval
- Teledyne Isco Dual 65DM fluid injection system with continuous flow
- Proppant slurry injection system
- Pressure, flow rate, temperature, strain, AE, and SP monitoring systems
- Post-test diamond cut cross section analysis for identifying created fracture geometry

This equipment has been subjected to preliminary calibration testing including a systems integration test and concept validation testing. The results of these tests and the subsequent analysis have provided data on produced hydraulic fracture geometry, small borehole sealing issues, and provided a general method for identifying borehole sealing failure as compared to brittle hydraulic fracture breakdown. In this method, a borehole seal failure may be identified by a decrease in the slope of the pressure-time curve before breakdown.

Also, a cross sectional analysis of the hydraulic fracture geometry provided some additional insight on the true complexity of hydraulic fractures as generated in nearly homogenous media. This analysis identified the growth of tangent fractures from the main hydraulic fracture as well as significant curvature. These observations may be relatable to near wellbore friction losses as considered in net pressure analysis.

REFERENCES

ASTM D4645 – 08 (2008), "Standard Test Method for Determination of In-Situ Stress in Rock Using Hydraulic Fracturing Method."

ASTM D7012 – 10 (2010), "Standard Test Method for Compressive Strength and Elastic Moduli of Intact Rock Core Specimens under Varying States of Stress and Temperatures."

ASTM D3967 – 08 (2008), "Standard Test Method for Splitting Tensile Strength of Intact Rock Core Specimens."

Beardsmore, G. R. and Cull, J. P. (2001), *Crustal Heat Flow: A Guide to Measurement and Modelling*, Cambridge University Press, Cambridge.

Behrmann, L. A. and Elbel, J. L. (1991), "Effect of Perforations on Fracture Initiation," In *Journal of Petroleum Technology*, Vol. 43, pp. 608-615.

Daneshy, A. A. (1973), "Experimental Investigation of Hydraulic Fracturing Through Perforations," In *Journal of Petroleum Technology*, Vol. 25, pp. 1201-1206, SPE 4333.

Dubynas, R. G. (1999), "Fracture Mechanics," In *Advanced Strength and Applied Stress Analysis*, Mogi, K. (2007). *Experimental Rock Mechanics*. Taylor & Francis Group, New York.

Franklin Well Service (2012), "Technical Information Sheet: Borate Cross-Link Fluid." Accessed at www.franklinwell.net on 01/10/2012.

Hunt, R. E. (2005), *Geological Engineering Site Investigation Handbook*, CRC Press.

Kumar, D. and Gutierrez, M. (2011), "Effects of Temperature on Two Dimensional Hydraulic Fracturing in Impermeable Rocks." Presented at the US Rock Mechanics / Geomechanics Symposium.

Rawlings, C. G., Barton, N. R., Bandis, S. C., Addis, M. A., and Gutierrez, M. S. (1993), "Laboratory and Numerical Discontinuum Modeling of Wellbore Stability," In *Journal of Petroleum Technology*, Vol. 45, pp. 1086-1092, SPE 25869.

Savić, M., Cockram, M. J., and Ziolkowski, A. M. (1993), "Active Ultrasonic Monitoring of Laboratory-Scale Hydraulic Fracturing Experiments: Numerical Modeling vs. Experiment," Presented at the Offshore European Conference, SPE 26793.

Second Edition, McGraw Hill: Boston, pp. 518 – 598.

Smith, C. G., Khait, S., and Albadraoui, D. (2008), "An Effective Technique to Reduce Bottomhole Friction Pressure During Hydraulic Fracturing Treatments," Presented at the SPE International Symposium and Exhibition on Formation Damage Control, SPE 112422.

Tester, J. W. et. al. (2006), "The Future of Geothermal Energy," Massachusetts Institute of Technology, ISBN: 0-615-13438-6.

Tsuyoshi, I., Chen, Q., Mizuta, Y., and Roegiers J.C. (2004), "Influence of Viscosity on the Hydraulic Fracturing Mechanism," In *Transactions of the ASME*, Vol. 126, pp. 190-200.

Valkó, P. and Economides, M. J. (1995), *Hydraulic Fracture Mechanics*, John Wiley & Sons.

ACKNOWLEDGEMENTS

Financial support provided by the U.S. Department of Energy under DOE Grant No. DE-FE0002760 is gratefully acknowledged. The opinions expressed in this paper are those of the authors and not the DOE.

APPENDIX

Systems integration testing pumping pressure-time plots are provided in appendix Figure A.1.

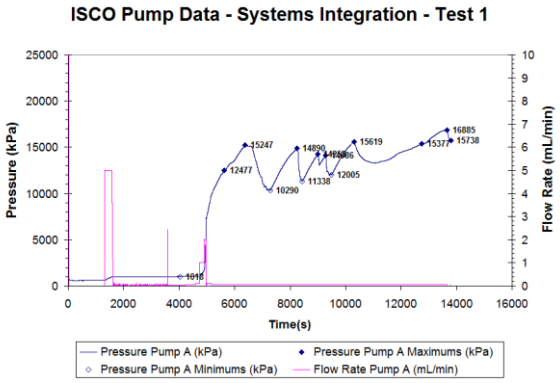

(a)

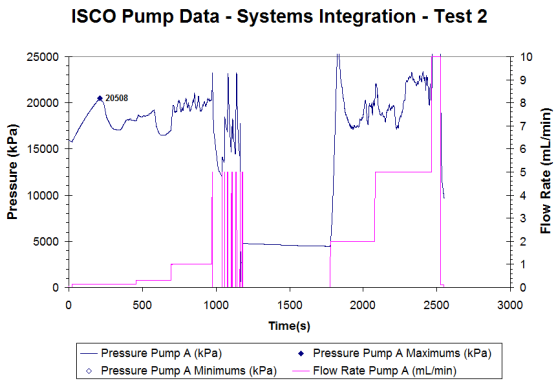

(b)

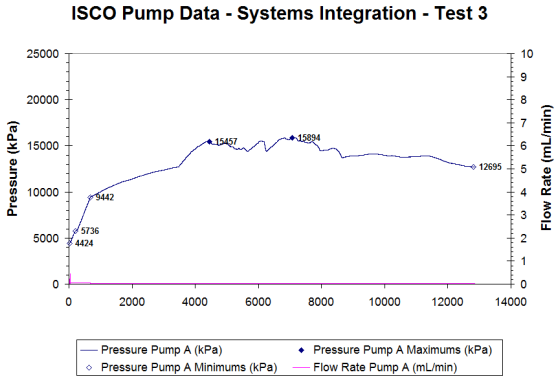

(c)

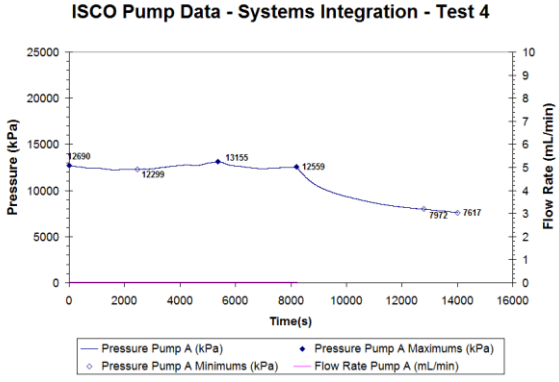

(d)

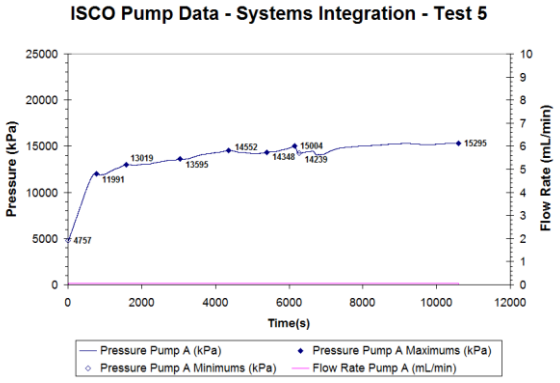

(e)

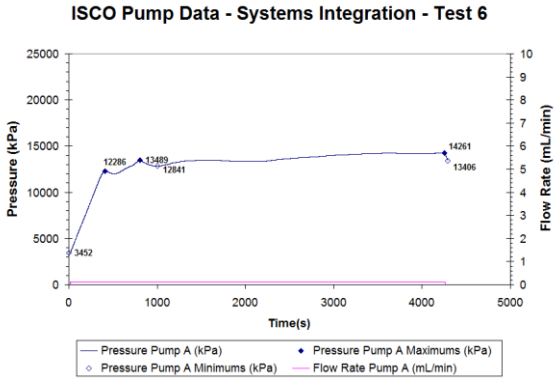

(f)

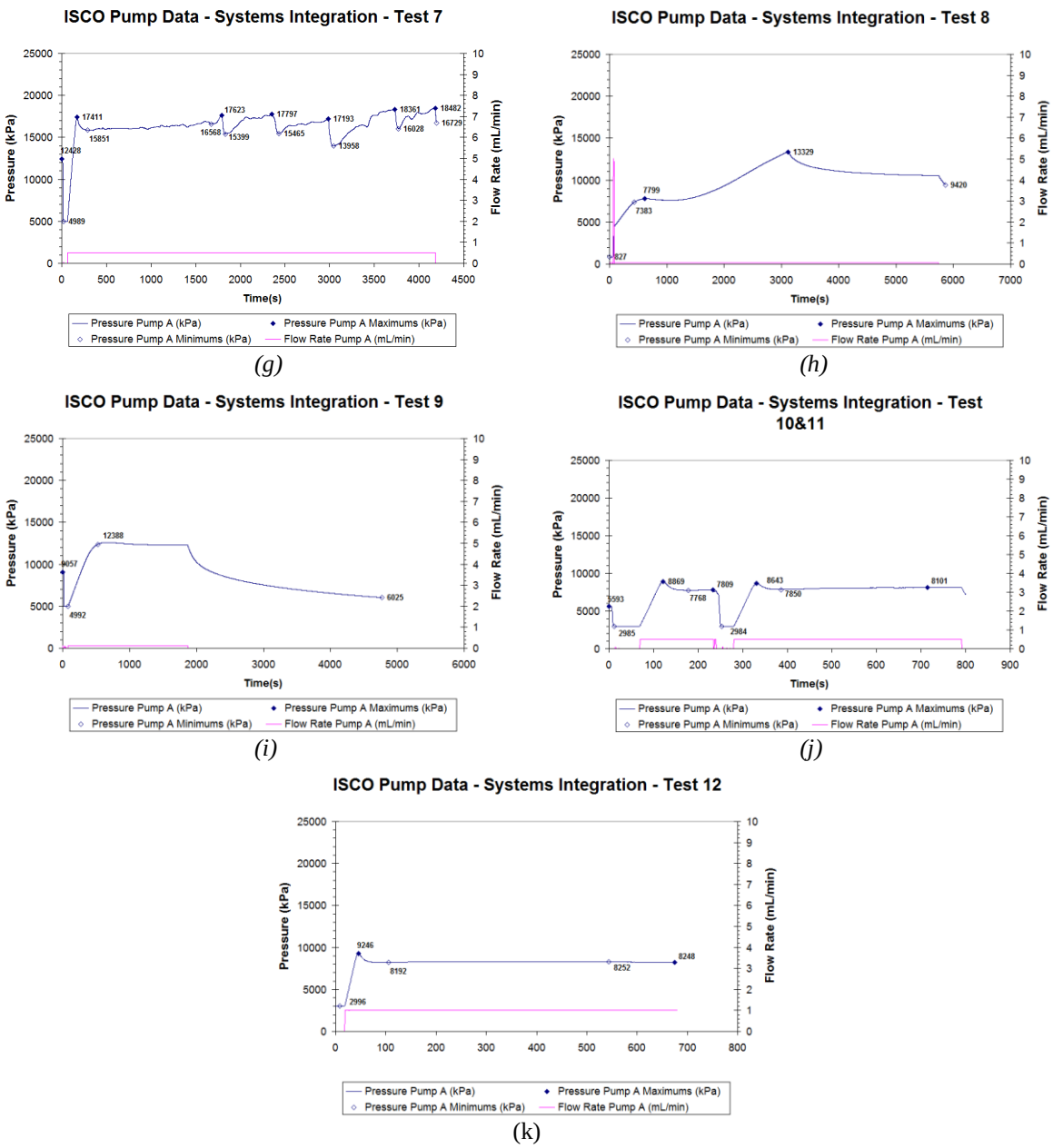

Figure A.1: Systems integration pumping pressure-time plots. (a) Test 1, (b) test 2, (c) test 3, (d) test 4, (e) test 5, (f) test 6, (g) test 7, (h) test 8, (i) test 9, (j) test 10 and 11, (k) test 12.